J Therm Anal Calorim (2017) 128:993–999
DOI 10.1007/s10973-016-6010-9

Trends in thermodynamic parameters of phase transitions of lanthanide sulfides $SrLnCuS_3$ (Ln = La–Lu)

Anna V. Ruseikina[1] · Oleg V. Andreev[1] · Eugenia O. Galenko[1] · Semyon I. Koltsov[1]

Received: 2 June 2016 / Accepted: 26 November 2016 / Published online: 19 December 2016

Abstract $SrLnCuS_3$ (Ln = La–Lu) compounds melt incongruently. Their thermochemical parameters are determined. The melting temperatures and the enthalpies of melting are: for $SrLaCuS_3$, $T = 1513$ K and $\Delta H = 6.9$ kJ mol^{-1}; for $SrCeCuS_3$, $T = 1468$ K and $\Delta H = 5.2$ kJ mol^{-1}; for $SrPrCuS_3$, $T = 1459$ K and $\Delta H = 13.2$ kJ mol^{-1}; for $SrNdCuS_3$, $T = 1429$ K and $\Delta H = 16.8$ kJ mol^{-1}; and for $SrSmCuS_3$, $T = 1605$ K and $\Delta H = 2.8$ kJ mol^{-1}. Three high-temperature polymorphic transitions are found to occur in $SrLnCuS_3$ (Ln = Sm, Gd–Lu) compounds. The parameters of these transitions are determined: for $SrSmCuS_3$, $T\alpha \leftrightarrow \beta = 1452$ K, $\Delta H\alpha \leftrightarrow \beta = 3.0$ kJ mol^{-1}, $T\beta \leftrightarrow \gamma = 1464$ K, $\Delta H\beta \leftrightarrow \gamma = 0.2$ kJ mol^{-1}, $T\gamma \leftrightarrow \delta = 1476$ K, and $\Delta H\gamma \leftrightarrow \delta = 1.1$ kJ mol^{-1}; for $SrDyCuS_3$, $T\alpha \leftrightarrow \beta = 1530$ K, $T\beta \leftrightarrow \gamma = 1568$ K, and $T\gamma \leftrightarrow \delta = 1585$ K; for $SrTmCuS_3$, $T\alpha \leftrightarrow \beta = 1580$ K, $T\beta \leftrightarrow \gamma = 1618$ K, and $T\gamma \leftrightarrow \delta = 1631$ K; and for $SrYbCuS_3$, $T\alpha \leftrightarrow \beta = 1567$ K, $T\beta \leftrightarrow \gamma = 1608$ K, and $T\gamma \leftrightarrow \delta = 1621$ K. The transitions are observed both upon heating and upon cooling. The high-temperature phases are not quenchable. Phase-transition temperature versus $r(Ln^{3+})$ curves for $SrLnCuS_3$ (Ln = La–Lu) feature the tetrad effect. The $SrLnCuS_3$ (Ln = La–Nd) compounds are classified as thiocuprates; their melting temperatures decrease systematically from La to Nd. The $SrCuLnS_3$ (Ln = Sm, Gd–Lu) compounds are classified as thiolanthanates; their melting temperatures increase in the order from Sm to Tm and from Tm to Lu.

✉ Anna V. Ruseikina
adeschina@mail.ru

[1] Institute of Chemistry, Tyumen State University, Tyumen, Russia

Keywords DSC · Incongruent melting · Lanthanide sulfides · Phase transitions

Introduction

Lanthanides and their salts have specific thermal, electric, and magnetic properties because of their peculiar electronic structure [1–4]. $A^{2+}Ln^{3+}Cu^{+}S_3$ (A = Pb, Eu, Sr, Ba) compounds are infrared and nonlinear optical materials [5, 6], p-type semiconductors with bandgap widths of 1.15–1.50 eV [7], or low-temperature ferrimagnets with ferrimagnetic transition temperatures of about 5.0 K [8, 9]. The constitution of $SrLnCuS_3$ compounds is like that of superconducting oxide ceramics [10]. The crystal-chemical parameters of $SrLnCuS_3$ (Ln = La–Lu) compounds were determined by X-ray powder diffraction [11–13]. Four types of orthorhombic structures exist in the $SrLnCuS_3$ series in the range 970–1170 K (Table 1). The $SrLnCuS_3$ (Ln = Pr, Nd) compounds have $BaLaCuS_3$ type structures (space group *Pnma*), the $SrLnCuS_3$ (Ln = Sm–Ho) compounds are isostructural to Eu_2CuS_3 (space group *Pnma*), and the $SrLnCuS_3$ (Ln = Er–Lu) compounds have $KZrCuS_3$ type structures (space group *Cmcm*) [11]. The $SrLnCuS_3$ (Ln = La, Ce) compounds each have two polymorphs: a low-temperature phase ($BaLaCuS_3$ type structure, annealing at 970 K) and a high-temperature phase (Ba_2MnS_3 type structure, annealing at 1170 K) [12]. These polymorphic transitions were not detected by differential thermal calorimetry (DSC) and were classified as slow transitions [11].

The following values of incongruent melting temperatures were reported for the title compounds: 1513 ± 2 for $SrLaCuS_3$ [13], 1486 ± 3 K for $SrCeCuS_3$ [12],

Table 1 Structure types of $SrLnCuS_3$ (Ln = La–Lu) compounds in the temperature range 970–1170 K

T/K	$SrLnCuS_3$ structure type [4, 10–13]												
	La	Ce	Pr	Nd	Sm	Gd	Tb	Dy	Ho	Er	Tm	Yb	Lu
1170										-	-	-	
1070		-					-		-		-	-	
970				-				-	-				

A vertically hatched cell denotes that the compound has a $BaLaCuS_3$ type structure; a crosshatched cell, a Eu_2CuS_3 type structure; a dark gray cell, a Ba_2MnS_3 type structure; a horizontally hatched cell, a $KZrCuS_3$ type structure; and a white cell with a hyphen , structure type not determined

1459 ± 2 K for $SrPrCuS_3$ [13], and 1703 ± 5 K for $SrHoCuS_3$ [14].

$SrLnCuS_3$ compounds are formed in the $LnCuS_2$–SrS sections of Cu_2S–Ln_2S_3–SrS quasi-ternary systems [11]. Other compounds formed in these systems (Cu_2S [15], Cu_3LnS_3 [16], and $LnCuS_2$ [17]) show high-temperature polymorphism. $EuGdCuS_3$, an isoformula compound, experiences three polymorphic transitions: $T\alpha \leftrightarrow \beta = 1460$ K, $\Delta H\alpha \leftrightarrow \beta = 2.6$ kJ mol^{-1}; $T\beta \leftrightarrow \gamma = 1492$ K, $\Delta H\beta \leftrightarrow \gamma = 2.3$ kJ mol^{-1}; and $T\gamma \leftrightarrow \delta = 1525$ K, $\Delta H\gamma \leftrightarrow \delta = 4.4$ kJ mol^{-1} [18]. Therefore, $SrLnCuS_3$ compounds are expected to show polymorphism in the range of temperatures from 1200 K to the melting point.

The tetrad or double–double effect is manifested in the lanthanide series, where the tetrads are La–Nd, Pm–Gd, Gd–Ho, and Er–Lu. The properties of lanthanide compounds within each tetrad are fitted by smooth functions. At the tetrad boundaries (which are crystal-chemical instability regions), singular points can appear on property versus lanthanide ionic radius $r(Ln^{3+})$ curves [19, 20].

The temperatures and enthalpies of phase transitions in $SrLnCuS_3$ (Ln = Nd–Dy, Er–Lu) compounds, their variation trends as a function of $r(Ln^{3+})$, and inner periodicities in the series of compounds remained undetermined until we undertook this study.

Our goals in this study were to determine the temperatures and enthalpies of phase transitions in $SrLnCuS_3$ (Ln = Nd, Sm, Gd–Dy, Er–Lu) compounds and to recognize the trends in phase-transition temperatures of $SrLnCuS_3$ (Ln = La-Lu) compounds as a function of $r(Ln^{3+})$.

Experimental

Cu_2S was prepared from constituent elements, which were specialty grade copper (os.ch. 11-4) and specialty grade sulfur (os.ch. 15-3), by ampoule synthesis. SrS was prepared by reacting $SrSO_4$ (a reagent grade sample) with H_2 at 1070 K for 15–20 h. Ln_2S_3 (Ln = Nd–Lu) sulfides were prepared from lanthanide oxides (HO-M, SmO-G, GdO-G, TbO-I, DiO-L, GoO-L, ErO-G, IbO-M, and LyuO-I types) in an H_2S and CS_2 flow at 1300 K [11]. The thus-prepared sulfides were single phases as probed by X-ray powder diffraction and were stoichiometric within the error bar of chemical analysis. $SrLnCuS_3$ samples were prepared by alloying the SrS, Ln_2S_3, and Cu_2S precursors taken in the ratio 2:1:1 in a graphite crucible that was mounted inside a degassed and sealed-off silica glass ampoule. The ampoule was heated in an electric furnace to 1570 K and then exposed at this temperature for 30 min. Cooling was in the switched-off mode. Samples were annealed at 970 K for 3 months [12, 21]. The as-annealed samples of compounds were single phases as probed by microstructure observations and X-ray powder diffraction. Their structure types are as shown in Table 1; their unit cell parameters agreed with reported values [11–13].

X-ray diffraction experiments were performed on a PANalytical X'Pert PRO diffractometer equipped with a PIXcel detector (CoK_α radiation, a graphite monochromator) and a DRON 7 diffractometer (CuK_α radiation, Ni filter) at 298 K. Powdery samples for use in these experiments were prepared by trituration with octane in an agate mortar. X-ray diffraction patterns were scanned at 298 K over the diffraction angle range $10° \le 2\theta \le 125$ (140)° in 0.013° steps with a total accumulation time of 13 h.

Differential scanning calorimetry experiments were performed on a Setsys Evolution 1750 (TG–DSC 1600) instrument using the Setsoft Software 2000 suite; the thermocouples were PtRh 6–PtRh 30%. The instrument was calibrated against the melting temperatures and heats of melting of references, which were Sn, Pb, Zn, Al, Ag, Au, Cu, and Pd [11]. The precision was within 0.5% in melting temperatures and within 10% in heats of melting. Samples for thermal analysis, weighing 99.3–109.6 mg, were cut to provide an as tight as possible fit to the lower portion of an alundum crucible ($V = 100$ μL). Programmed heating was at a rate of 5 K min^{-1}. Prior to an experiment, the working chamber of the instrument was degassed and filled with argon. The purging gas flow rate

during an experiment was 25 mL min^{-1}. The values of three replicate temperature or heat measurements fell within the error bars of thermal analysis. When the thermoanalytical experiment reached 1840 K, samples melted completely.

Microstructure was observed on polished samples using an AxioVert.A1 microscope. The Edstate 2D software was used for graphic representation.

Distribution spectra of chemical elements were measured at five spots of the surface of a $SrLnCuS_3$ sample using a JEOL JSM-6510 LM scanning electron microscope (Fig. 1) to determine the compositional homogeneity of the samples. Color difference does not signify compositional inhomogeneity of a sample, but rather is a characteristic feature of topographic contrast in SEM images, a higher brightness of peaks and protrusions of the relief (the edge effect) [22, 23]. The results of X-ray spectral microanalysis of $SrLnCuS_3$ samples coincided with calculated values within the measurement error of ±0.5 mass% (Table 2).

Table 2 Elements surface distribution in a $SrYbCuS_3$ sample as probed by X-ray spectral microanalysis

Sr		Yb		Cu		S	
m_{calcd}	m_{found}	m_{calcd}	m_{found}	m_{calcd}	m_{found}	m_{calcd}	m_{found}
20.85	21.31	41.18	40.80	15.12	15.25	22.85	22.64

m_{calcd} and m_{found} are, respectively, the calculated mass percentage and the as-analyzed mass percentage of an element in $SrYbCuS_3$

Results and discussion

$SrLnCuS_3$ (Ln = La–Lu) are incongruently melting compounds. The thermal events associated with melting of these compounds in $SrLnCuS_3$–SrS quasi-binary sections appear at constant temperatures, which is verified by the construction of Tammann's triangle. Initially, single-phase samples become multiphase when melted and solidified again. Polished cross sections of the solidified samples show SrS primary grains surrounded by $SrLnCuS_3$ crystals. In between grains, there are narrow fields of the eutectic formed by $LnCuS_2$ and $SrLnCuS_3$ phases. The eutectic solidification peak appears on DSC cooling curves. The X-ray diffraction patterns of solidified samples feature reflections from $SrLnCuS_3$, SrS, and $LnCuS_2$ phases.

The DSC heating curves for single-phase $SrLnCuS_3$ (Ln = La, Ce, Pr, Nd) samples feature distinct endotherms of incongruent melting of $SrLnCuS_3$ (Fig. 2). Melting peaks of the SrS crystals that are formed upon incongruent $SrLnCuS_3$ decomposition, are not distinct on the heating curves. Some DSC cooling curves feature exotherms due to crystallization of SrS primary crystals. The decrease in incongruent melting temperatures of $SrLnCuS_3$ (Ln = La–Nd) compounds as a function of $r(Ln^{3+})$ (Table 3, Fig. 3) signifies a decline in the thermodynamic stability of these compounds in the series from La to Nd.

In going from $SrNdCuS_3$ to $SrSmCuS_3$, the structure changes from $BaLnCuS_3$ type in $SrNdCuS_3$ to Eu_2CuS_3 type in $SrSmCuS_3$, and the coordination polyhedron changes from a one-capped trigonal prism NdS_7 to an octahedron SmS_6 [11]. The character of $SrLnCuS_3$ compounds and their thermal characteristics also change fundamentally in going from $SrNdCuS_3$ to $SrSmCuS_3$.

DSC heating curves feature three high-temperature endotherms (1450–1650 K) for each $SrLnCuS_3$ (Ln = Sm, Gd–Lu) compound (Fig. 2; Table 3). These endotherms are completely reproduced upon cooling. Peak shapes have a well-defined linear portion. The relevant phase transitions occur within a narrow temperature window (5–10 K on the average). Similar shapes are intrinsic to the phase transitions that appear as invariant phase equilibria in phase diagrams [24]. The enthalpies of the first phase transition in the $SrLnCuS_3$ (Ln = Sm, Gd–Lu) compounds fall in the range ΔH = 2.4–9.7 kJ mol^{-1}, those of the second transition are ΔH = 0.2–3.9 kJ mol^{-1}, and for the third transition, ΔH = 0.5–3.7 kJ mol^{-1}. After the third endotherm, a $SrLnCuS_3$ sample remains polycrystalline; no liquid phase appears. The thermal features are completely

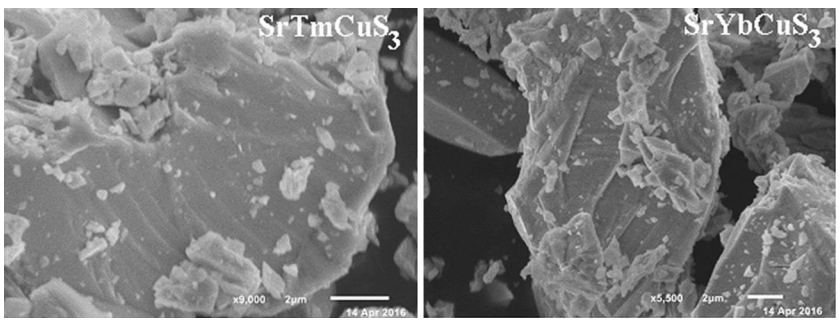

Fig. 1 SEM micrographs of $SrLnCuS_3$ (Ln = Tm, Yb) samples

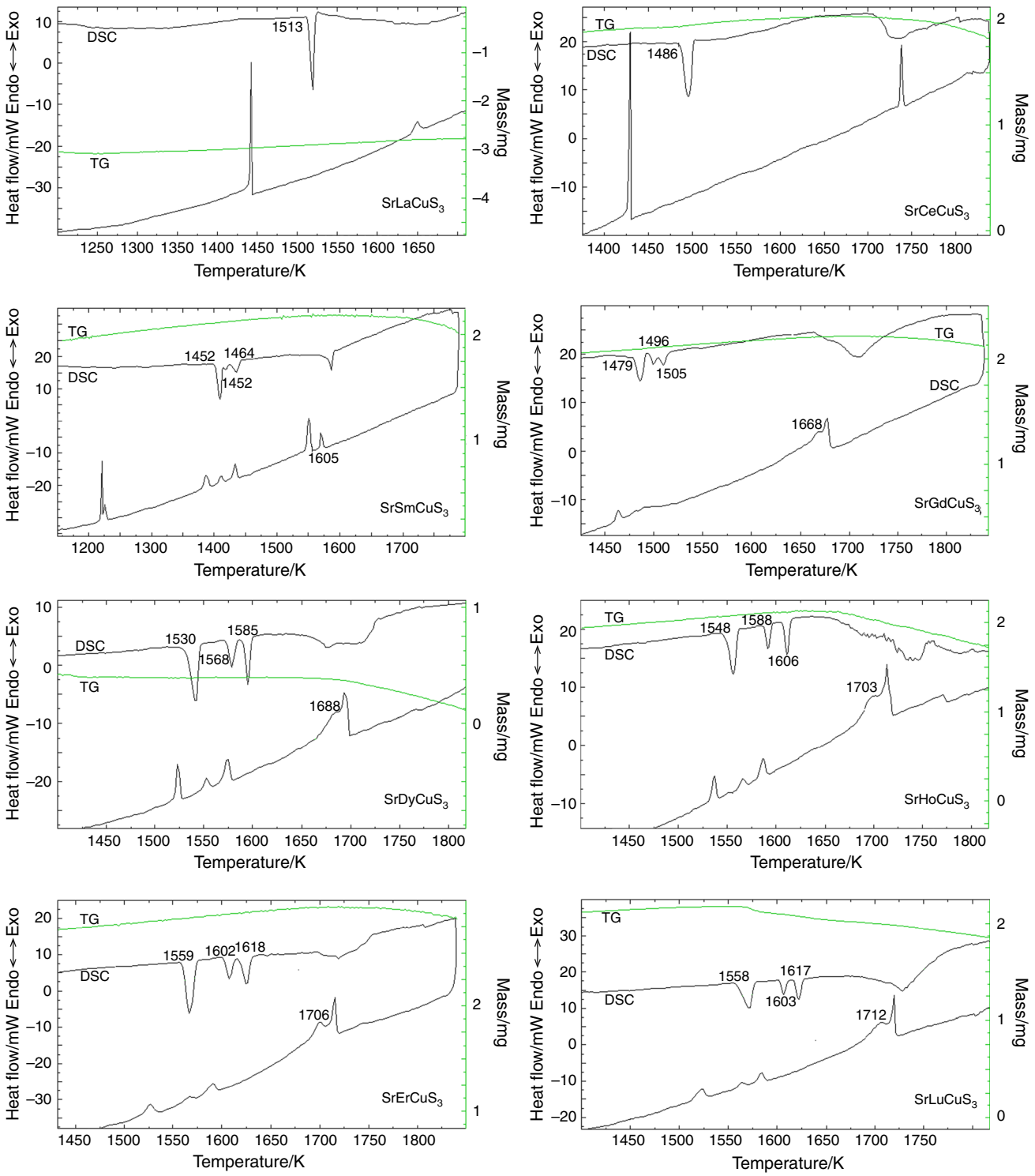

Fig. 2 Thermal curves for samples of $SrLnCuS_3$ (Ln = La [10], Ce [9], Ho [11], for the Sm, Dy, Er, and Lu compounds; the curves were measured in this work)

reproduced in several heating–cooling cycles. The sample cooled after being thermocycled is a single phase and has its intrinsic crystal structure (Table 1). DSC data imply that $SrLnCuS_3$ compounds experience first-order phase (polymorphic) transitions.

Since these transitions are detected by a DSC method both upon heating and upon cooling, they may be regarded to be rapid transitions [24]. High-temperature phases of $SrLnCuS_3$ (Ln = Sm, Gd–Lu) were not quenchable at cooling rates of $\sim 10^3$–10^4 K min^{-1}.

Table 3 Temperatures and enthalpies of high-temperature phase transitions in $SrLnCuS_3$ (Ln = La–Lu) compounds

Compound	Temperatures and enthalpies of phase transitions							
	$\alpha \leftrightarrow \beta$		$\beta \leftrightarrow \gamma$		$\gamma \leftrightarrow \delta$		T_m/K	ΔH_m/kJ mol^{-1}
	T/K	ΔH/kJ mol^{-1}	T/K	ΔH/kJ mol^{-1}	T/K	ΔH/kJ mol^{-1}		
$SrLaCuS_3$ [1]	–	–	–	–	–	–	1513 ± 2	6.9 ± 0.6
$SrCeCuS_3$ [2]	–	–	–	–	–	–	1486 ± 3	5.2 ± 0.6
$SrPrCuS_3$ [1]	–	–	–	–	–	–	1459 ± 2	13.2 ± 1.2
$SrNdCuS_3$	–	–	–	–	–	–	1429 ± 6	16.8 ± 1.9
$SrSmCuS_3$	1452 ± 2	3.0 ± 0.3	1464 ± 6	0.2 ± 0.02	1476 ± 4	1.1 ± 0.1	1605 ± 5[a]	2.8 ± 0.3[a]
$SrGdCuS_3$	1479 ± 4	2.4 ± 0.2	1496 ± 3	0.4 ± 0.04	1505 ± 2	0.5 ± 0.04	1668 ± 4[b]	–
$SrTbCuS_3$	1512 ± 3	5.4 ± 0.6	1551 ± 2	3.9 ± 0.4	1566 ± 3	1.3 ± 0.1	–	–
$SrDyCuS_3$	1530 ± 5	2.9 ± 0.3	1568 ± 6	1.0 ± 0.1	1585 ± 5	1.5 ± 0.2	1688 ± 7[b]	–
$SrHoCuS_3$ [3]	1548 ± 2	2.8 ± 0.3	1588 ± 2	1.0 ± 0.1	1606 ± 2	1.5 ± 0.1	1703 ± 5[a]	–
$SrErCuS_3$	1558 ± 1	2.9 ± 0.3	1601 ± 1	0.7 ± 0.1	1617 ± 2	1.0 ± 0.1	1706 ± 8[b]	–
$SrTmCuS_3$	1580 ± 2	9.7 ± 0.9	1618 ± 2	2.4 ± 0.2	1631 ± 1	3.7 ± 0.4	1678 ± 5[a]	–
$SrYbCuS_3$	1567 ± 5	7.1 ± 0.7	1608 ± 7	2.2 ± 0.2	1621 ± 5	3.2 ± 0.3	1695 ± 6[b]	–
$SrLuCuS_3$	1558 ± 4	3.9 ± 0.4	1603 ± 4	1.0 ± 0.1	1617 ± 2	1.6 ± 0.2	1712 ± 6[b]	–

[a] The value derived from the cooling curve

[b] The average of values derived from the cooling curve and heating curve

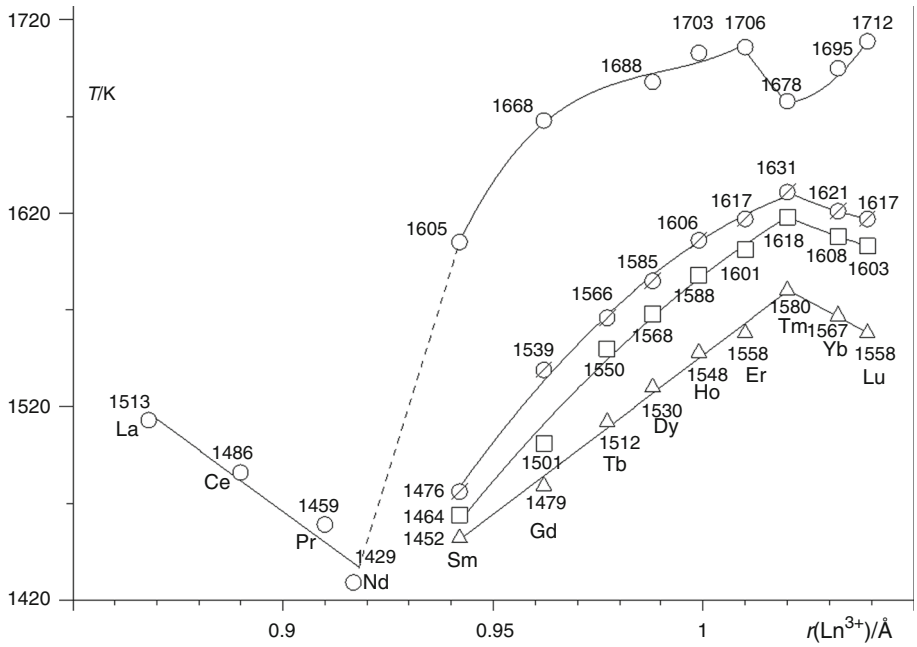

Fig. 3 Phase-transition temperatures of $SrLnCuS_3$ (Ln = La–Lu) compounds along the lanthanide series: $\Delta\alpha \rightarrow \beta$, $\square \rightarrow \gamma$, and $\varnothing\ \gamma \rightarrow \beta$ polymorphic transitions and incongruent melting

The compounds melt near the liquidus temperatures of the relevant systems. The peaks of incongruent melting of $SrLnCuS_3$ and those of melting of SrS crystals are superimposed on each other both upon heating and upon cooling. The incongruent melting peak for $SrSmCuS_3$ is distinct enough to make it possible to determine the enthalpy of melting (Table 3). In the $SrLnCuS_3$ compounds of heavier lanthanides (Ln = Gd–Lu), the melting peak is blurred and appears distinctly only upon cooling, immediately following the exotherm of crystallization of SrS primary grains. Table 3 shows the values of incongruent melting temperatures of $SrLnCuS_3$ compounds and the liquidus temperatures derived from heating and cooling curves and averaged.

Table 4 Onset mass loss temperatures (T_{on}) for $SrLnCuS_3$ (Ln = Dy–Lu) samples

Composition prior to DSC	T_m/K	T_{on}/K	Δm/mass%	Composition after DSC
$SrDyCuS_3$	1688	1692	–	$SrDyCuS_3$
$SrHoCuS_3$	1703	1665	0.1	$SrHoCuS_{2.99}$
$SrErCuS_3$	1706	1719	–	$SrErCuS_3$
$SrTmCuS_3$	1678	1740	–	$SrTmCuS_3$
$SrYbCuS_3$	1695	1577	0.2	$SrYbCuS_{2.98}$
$SrLuCuS_3$	1712	1561	0.2	$SrLuCuS_{2.97}$

The $SrLnCuS_3$ (Ln = La–Dy, Tm) compounds are thermally stable phases. Samples of $SrLnCuS_3$ (Ln = La–Nd, Sm, Gd, Dy, Er, Tm) compounds experience mass loss after they melt incongruently and a liquid phase appears (Table 4). The $SrLnCuS_3$ (Ln = Ho, Yb, Lu) compounds experience a 0.1–0.2% mass loss at temperatures below their incongruent melting temperatures to become nonstoichiometric. No accessory phases were detected in their samples. Compositions of the compounds were calculated on the assumption that the mass loss arose from partial vaporization of sulfide sulfur.

The decreasing trend in thermal stabilities of $SrLnCuS_3$ compounds along the Ln series from La to Nd and their increasing trend from Sm to Tm and from Tm to Lu can qualitatively be interpreted in terms of the acidity–basicity of the constituent simple sulfides [24]. $SrLnCuS_3$ compounds are formed by SrS (a basic sulfide) and by Cu_2S and Ln_2S_3, which are acidic relative to SrS. The acidity of Ln_2S_3 increases in the lanthanide series as the ionic radius $r(Ln^{3+})$ decreases [25] and the electronegativity of lanthanide atoms increases (XLa = 1.27, XNd = 1.33, XGd = 1.42, XDy = 1.43, XHo = 1.47, and XTm = 1.48 [26]) [24]. For the elements of the first tetrad (La–Nd), Cu_2S exceeds Ln_2S_3 in acidity. The $SrLnCuS_3$ (Ln = La–Nd) compounds are classified as thiocuprates. The strengthening acidities of sulfides in the order from La_2S_3 to Nd_2S_3 are responsible for the decreasing trend in thermal stabilities of the relevant thiocuprates. All $SrCuLnS_3$ compounds with heavier lanthanides are treated as thiolanthanates. The thermal stabilities of thiolanthanates increase in proportion to the strengthening acidities of Ln_2S_3. The singularity appearing at Tm on the phase-transition curves correlates with the filling-in of the 4*f* level in Tm ($4f^{13}5d^06s^2$), in Yb ($4f^{14}5d^06s^2$), and in Lu ($4f^{14}5d^16s^2$).

The tetrad effect is manifested in the $SrLnCuS_3$ (Ln = La–Lu) series. Structural studies showed that the structure type of the orthorhombic $SrLnCuS_3$ phase changes in going from Nd to Sm and from Ho to Er [11, 14] at 1170 K. $SrNdCuS_3$ has a $BaLaCuS_3$ type structure, which transforms to Eu_2CuS_3 type in $SrSmCuS_3$, and the latter exists in the series of compounds through $SrCuHoS_3$ [11]. $SrCuErS_3$ has a $KZrCuS_3$ type structure [11]. The fitting polynomial of the incongruent melting temperature versus $r(Ln^{3+})$ curve for $SrCuLnS_3$ compounds changes in going from Nd to Sm. High-temperature polymorphs appear in the $SrCuLnS_3$ (Ln = Sm, Gd–Lu) compounds. The effect of filling-in of the 4*f* level is manifested in going from the Tm to Yb compound.

Conclusions

$SrLnCuS_3$ compounds (Ln = La–Lu) show polymorphism and incongruent melting. Four types of orthorhombic structures exist in the $SrLnCuS_3$ series in the range 970–1170 K. DSC data imply that $SrLnCuS_3$ compounds (Ln = Sm–Lu) experience first-order phase (polymorphic) transitions in range of 1460–1630 K both upon heating and upon cooling. There is an increase in phase-transition temperatures of $SrLnCuS_3$ for Ln = Sm–Tm compounds and a decrease in them for Yb and Lu. The enthalpies range from 0.2 to 9.7 kJ mol^{-1}. There is linear decrease in incongruent melting temperatures of $SrLnCuS_3$ (Ln = La–Nd) compounds as a function of $r(Ln^{3+})$. Temperatures range from 1513 K (ΔH = 6.9 kJ mol^{-1}) for La to 1429 (ΔH = 16.8 kJ mol^{-1}) for Nd. Compounds are classified as thiocuprates. The thermal stabilities of $SrLnCuS_3$ compounds in the order from Sm (1605 K) to Er (1708 K) increase in proportion to the strengthening acidities of Ln_2S_3. Compounds are treated as thiolanthanates.

Acknowledgements This study was financially supported by the assignment of the Russian Federation Government No. 2014/228 (R&D Project No. 996) and by the Engineering Center of Tyumen State University as a pilot project in the frame of the Engineering Roadmap approved by the Russian Federation Government in Decree No. 1300-r, July 23, 2013; and the State Program of the Russian Federation "Development of Industries and Improvement of Their Competitiveness" approved by the Russian Federation Government in Resolution No. 328, April 15, 2014.

References

1. Zapała L, Kosińska M, Woźnicka E, Byczyński L, Zapała W. Synthesis, spectral and thermal study of La(III), Nd(III), Sm(III), Eu(III), Gd(III) and Tb(III) complexes with mefenamic acid. J Therm Anal Calorim. 2016;124(1):363–74.
2. Xia Y, Huang Y, Li Y, Liao S, Long Q, Liang J. LaPO4: Ce, Tb, Yb phosphor—synthesis and kinetics study for thermal process of precursor by Vyazovkin, OFW, KAS, Starink, and Mastplosts methods. J Therm Anal Calorim. 2015;120(3):1635–43.
3. Rojas RM, Torralvo MJ, Otero-Diaz LC. Thermal behaviour and microstructural characterization of lanthanide sulphides. J Therm Anal Calorim. 1992;38(4):961–71.
4. Koscielski LA, Ibers JA. The structural chemistry of quaternary chalcogenides of the type AMM'Q_3. Z Anorgan Allgem Chem. 2012;638(B.15):2585–93.
5. Gylay LD, Olekseyuk ID, Wolcyrz M, Stepien-Damm J. Crystal structures of the $RCuPbS_3$ (R = Tb, Dy, Ho, Er, Tm, Yb and Lu) compounds. J Alloys Compd. 2005;399:189–95.
6. Gulay LD, Shemet VY, Olekseyuk ID, Stepie-Damm J, Pietraszko A, Koldun LV, Filimonyuk JO. Investigation of the R_2S_3–Cu_2S–PbS (R = Y, Dy, Ho and Er) systems. J Alloys Compd. 2007;431:77–84.
7. Brennan TD, Ibers JA. $LaPbCuS_3$: Cu(I) insertion into the α-La_2S_3 framework. J Solid State Chem. 1992;97:377–82.
8. Wakeshima M, Furuuchi F, Hinatsu Y. Crystal structures and magnetic properties of novel rare-earth copper sulfides, $EuRCuS_3$ (R = Y, Gd–Lu). J Phys: Condens Matter. 2004;16:5503–18.
9. Furuuchi F, Wakeshima M, Hinatsu Y. Magnetic properties and (151)Eu Mossbauer effects of mixed valence europium copper sulfide, Eu_2CuS_3. J Solid State Chem. 2004;177(11):3853–8.
10. Sikerina NV. Regularities of phase equilibria in the SrS–Cu_2S–Ln_2S_3 (Ln = La–Lu) systems, preparation and composition of $SrLnCuS_3$ compounds (Cand. Diss. thesis): Tyumen. 2005:26.
11. Andreev OV, Ruseikina AV, Solovyev LA, Bamburov VG. Synthesis, structure, physicochemical characteristics of $ALnBS_3$ (A = Sr, Eu; Ln = La–Lu; B = Cu, Ag). Ekaterinburg: EPD UD RAS;2014.
12. Ruseikina AV, Solov'ev LA. Crystal structures of α- and β-$SrCeCuS_3$. Russ J Inorg Chem. 2016;61(4):482–7.
13. Ruseikina AV, Solov'ev LA, Andreev OV. Crystal structures and properties of $SrLnCuS_3$ (Ln = La, Pr). Russ J Inorg Chem. 2014;59(3):196–201.
14. Ruseikina AV, Koltsov SI, Tupitcyn AV. Synthesizing a new complex sulfide $SrHoCuS_3$. In: XV international scientific conference «High-Tech in Chemical Engineering—2014», Zvenigorod M, editors. Lomonosow Moscow State University of Fine Chemical Technologies (MITHT Publisher). 2014;215 (**in Russian**).
15. Cook W, Shiozawa L, Augustine F. The Cu–S phase diagram. J Appl Phys. 1970;41:3058–63.
16. Ballestracci R, Bertaut EF. Etude cristallographigue de nouveaux sulfures des terres rares et de cuivre (1). Bull Soc Fransc Miner Crist. 1965;88(4):575–9.
17. Andreev OV, Ruseikina AV. Heat of melting compounds $LnCuS_2$. Tyumen State Univ Her. 2011;5:186–9.
18. Ruseikina AV, Demchuk ZA, Kislitcyn AA. Warmth of phase transformations connection of $EuGdCuS_3$. Tyumen State Univ Her. 2012;5:19–25.
19. Dzhurinskii BF, Bandurkin GA. Lanthanon pereodic behaviour and inorganic materials [Pereodichnost' svoystv lantanidov i neorganicheskie materialy]. Neorg Mater. 1979;15(6):1024–7 (**in Russian**).
20. Dzhurinskii BF. Rare earth element periodic behaviour [Pereodichnost' svoystv redkozemelnyh elementov]. Russ J Inorg Chem. 1980;25(1):79–86 (**in Russian**).
21. Fedorov PP. Anneal time determined by studying phase transitions in solid binary systems. Russ J Inorg Chem. 1992;37(8):1891–4.
22. Clarke A, Eberhardt C. Microscopy techniques for materials science. Cambridge: Woodhead Publishing; 2002.
23. Brandon DG, Kaplan WD. Microstructural characterization of materials. London: Wiley; 1999.
24. Andreev OV, Bamburov VG, Monina LN, Razumkova IA, Ruseikina AV, Mitroshin OYu, Andreev VO. Phase equilibria in the sulfide systems of the 3d-, 4f-elements. Ekaterinburg: EPD UD RAS;2015.
25. Shannon RD. Revised effective ionic radii and systematic studies of interatomic distances in halides and chalcogenides. Acta Crystallogr. 1976;32:751–67.
26. Husain M, Batra A, Srivastava KS. Electonegative, radii elements. Polyhedron. 1989;8(9):1233–4.